

# UC San Diego

## UC San Diego Previously Published Works

### Title

Recurrent homozygous damaging mutation in TMX2, encoding a protein disulfide isomerase, in four families with microlissencephaly

### Permalink

<https://escholarship.org/uc/item/7f55k9s5>

### Journal

Journal of Medical Genetics, 57(4)

### ISSN

0022-2593

### Authors

Ghosh, Shereen Georges  
Wang, Lu  
Breuss, Martin W  
[et al.](#)

### Publication Date

2020-04-01

### DOI

10.1136/jmedgenet-2019-106409

Peer reviewed



Published in final edited form as:

*J Med Genet.* 2020 April ; 57(4): 274–282. doi:10.1136/jmedgenet-2019-106409.

## Recurrent Homozygous Damaging Mutation in *TMX2*, Encoding a Protein Disulfide Isomerase, in Four Families with Microlissencephaly

Shereen G. Ghosh<sup>1,2</sup>, Lu Wang<sup>1,2</sup>, Martin W. Breuss<sup>1,2</sup>, Joshua D. Green<sup>3</sup>, Valentina Stanley<sup>1,2</sup>, Xiaoxu Yang<sup>1,2</sup>, Danica Ross<sup>1,2</sup>, Bryan J. Traynor<sup>3,4</sup>, Amal Alhashem<sup>5</sup>, Matloob Azam<sup>6</sup>, Laila Selim<sup>7</sup>, Laila Bastaki<sup>8</sup>, Hanan I. Elbastawisy<sup>9</sup>, Samia Temtamy<sup>10</sup>, Maha S. Zaki<sup>11</sup>, Joseph G. Gleeson<sup>1,2,\*</sup>

<sup>1</sup>Department of Neurosciences, Howard Hughes Medical Institute, University of California, San Diego, La Jolla, CA 92093, USA

<sup>2</sup>Rady Children's Institute for Genomic Medicine, San Diego, CA 92025, USA

<sup>3</sup>Neuromuscular Diseases Research Section, Laboratory of Neurogenetics, NIA, NIH, Bethesda, MD 20892, USA

<sup>4</sup>Neurology Department, Johns Hopkins University, Baltimore, MD 21287, USA

<sup>5</sup>Department of Pediatrics, Prince Sultan Medical Military City, Riyadh 12233, Saudi Arabia

<sup>6</sup>Department of Pediatrics and Child Neurology, Wah Medical College, Wah Cantt, 47040 Pakistan

<sup>7</sup>Pediatric Neurology Department, Cairo University, Cairo 12613, Egypt

\*Please address correspondence to: Joseph G. Gleeson, Department of Neurosciences, University of California, San Diego, 92093, USA; jogleeson@ucsd.edu.

**Contributors:** Contributors SGG and JGG conceptualized the study. SGG, LW, MB, JDG, XY, DR, and BJT performed the experiments and/or conducted analyses for the figures. VS, AA, MA, LS, LB, HA, MSZ, and JGG provided clinical information to conduct the study. JGG supervised the study. SGG and JGG wrote the original manuscript. All authors contributed to revisions and approved the final version.

**Competing Interests:** The authors declare no conflict of interest.

**Data availability:** Data are available in a public, open access repository. The exome sequencing data from individuals from the University of California, San Diego, study site have been deposited in the Database of Genotypes and Phenotypes under accession number dbGaP:phs000382.v1.p1.

### WEB RESOURCES

RefSeq, <http://www.ncbi.nlm.nih.gov/RefSeq>

Online Mendelian Inheritance in Man (OMIM), <http://www.omim.org>

HomozygosityMapper, <http://www.homozygositymapper.org/>

Mutation Taster, <http://www.mutationtaster.org/>

Exome aggregation Consortium, ExAc Browser <http://exac.broadinstitute.org/>

1000 Genomes, <http://browser.1000genomes.org>

GME Variome, <http://igm.ucsd.edu/gme>

The Genotype-Tissue Expression (GTEx) Project, <https://www.gtexportal.org/home/>

BrainSpan – Atlas of the Developing Human Brain, <http://www.brainspan.org/>

Human Splicing Finder, <http://www.umd.be/HSF/>

UCSC Genome Browser, <https://genome.ucsc.edu/>

SimulConsult – Measurement resources, <http://www.simulconsult.com/resources/measurement.html>

Python Software Foundation, <https://www.python.org/>

NCBI database of Genotypes and Phenotypes (dbGaP), <http://www.ncbi.nlm.nih.gov/gap>

UniProt, <https://www.uniprot.org/>

<sup>8</sup>Kuwait Medical Genetics Centre, Sabah Health District, Shuwaikh 44000, Kuwait

<sup>9</sup>Department of Ophthalmic Genetics, Research Institute of Ophthalmology, Sulaibikhat 12557, Egypt

<sup>10</sup>Center of Excellence for Human Genetics, National Research Centre, Cairo 12622, Egypt

<sup>11</sup>Clinical Genetics Department, Human Genetics and Genome Research Division, National Research Centre, Cairo 12622, Egypt

## Abstract

**Background**—Protein Disulfide Isomerase (PDI) proteins are part of the Thioredoxin (TRX) protein superfamily. PDIs are involved in the formation and rearrangement of disulfide bonds between cysteine residues during protein folding in the endoplasmic reticulum (ER) and are implicated in stress response pathways.

**Methods**—Eight children from four consanguineous families residing in distinct geographies within the Middle East and Central Asia were recruited for study. All probands showed structurally similar microcephaly with lissencephaly (microlissencephaly) brain malformations. DNA samples from each family underwent whole exome sequencing (WES), assessment for repeat expansions, and confirmatory segregation analysis.

**Results**—An identical homozygous variant in *TMX2* (c.500G>A), encoding Thioredoxin-related transmembrane protein 2, segregated with disease in all four families. This variant changed the last coding base of exon six, and impacted mRNA stability. All patients presented with microlissencephaly, global developmental delay, intellectual disability, and epilepsy. While *TMX2* is an activator of cellular *C9ORF72* repeat expansion toxicity, patients showed no evidence of *C9ORF72* repeat expansions.

**Conclusion**—The *TMX2* c.500G>A allele associates with recessive microlissencephaly, and patients show no evidence of *C9ORF72* expansions. *TMX2* is the first PDI implicated in a recessive disease, suggesting a protein isomerization defect in microlissencephaly.

## Keywords

*TMX2*; thioredoxin; ER stress; microlissencephaly; protein disulfide isomerase

## INTRODUCTION

Lissencephaly (LIS, lissos means smooth in Greek) refers to a smooth surface of the cerebral cortex.[1] Previously termed ‘type I’ and ‘type II’ to refer to the absence or presence of coexistent microcephaly,[1] respectively, recent lissencephaly molecular classification has identified eight recurrently mutated genes in recessive forms of disease: *RELN* (MIM:600514), *NDE1* (MIM:609449), *LAMB1* (MIM:150240), *KATNB1* (MIM:602703), *CDK5* (MIM:123831), *TMTC3* (MIM:617218).[2–7] Primary microcephaly (MPCH) refers to reduced head size with reduced cerebral volume; and at the more severe end of the spectrum, there is often a reduction in the complexity of the folding of the cerebral cortex, termed ‘simplified gyral pattern.’[8] Therefore, most cases with microcephaly show only mild disruption of the gyral folding on brain MRI, but at the severe end of microcephaly

spectrum the cerebral cortex can show gyri paucity, and can be difficult to distinguish from forms of lissencephaly. A distinct entity termed ‘microlissencephaly’ describes the combination of lissencephaly with microcephaly.[9] Of the recessive causes for lissencephaly only a few show notable additional microcephaly: *RELN*, *NDE1*, *KATNB1*, and a few chromosomal deletion syndromes.[2, 3, 5, 10] This suggests the existence of genetic conditions in which the degree of lissencephaly is greater than would be expected from the degree of microcephaly alone, supporting the use of the term microlissencephaly for appropriate conditions.

Some genes linked to microcephaly with lissencephaly, such as *TMTC3*, are implicated in the endoplasmic reticulum (ER) stress response, which is activated upon misfolding of secretory proteins or calcium balance perturbation.[11,12] Overload of ER protein folding capacity can lead to an accumulation of misfolded proteins, ER stress and subsequent cell death. Protein disulfide isomerases (PDIs) are resident transmembrane ER proteins that catalyze thiol-disulfide interchanges, which are critical for proper protein folding.[13] There are 21 known genes encoding PDIs, including three members of the Thioredoxin-related transmembrane (TMX) family, TMX-1 (MIM:610527), -2 (MIM:616715), and -3 (MIM:616102). Each TMX family member encodes an N-terminal signal peptide, single-pass transmembrane domain, C-terminal thioredoxin (Trx)-like domain, and a Di-lysine ER retention signal domain, but how they maintain protein homeostasis in the ER remains unknown.[14]

## METHODS

### Patient recruitment

The procedures followed for recruitment and data collection were in accordance with the ethical standards of the responsible committee on human experimentation at the University of California, San Diego.

### DNA extraction and whole exome sequencing

This study was approved by the Institutional Review Board at the respective host institution. All study participants and/or their guardians signed informed consents, and the study was performed in accordance with Health Insurance Portability and Accountability Act (HIPAA) Privacy Rules. DNA was extracted from peripheral blood leukocytes with salt extraction. DNA from the probands was subjected to Agilent Sure-Select Human All Exon v2.0 (44Mb target) and Illumina Rapid Capture Enrichment (37Mb target) library preparation and sequenced on Illumina HiSeq 2000 or 4000 instruments.[15]

### Computational analysis

Variant calling and filtering were performed according to a previously described whole exome sequencing pipeline.[15] Variants were filtered if not present in all affected individuals in the family, with zygosity based upon the presumed mode of inheritance. For all families, variants were filtered for minor allele frequency (MAF) >1:1000, PolyPhen-2 scores of <0.9 or GERP score <4.5. Variants were assessed with MutationTaster, and runs of homozygosity were defined with HomozygosityMapper.[16–18]

### **TMX2 mRNA assessment**

Total RNA was extracted from fresh frozen blood on available parents and probands using TRIzol™, quantified by spectrophotometry, and reverse-transcribed using the Superscript III First-Strand cDNA Kit (Invitrogen). PCR analysis of cDNA was performed using dHPLC-purified primers (see supplementary table S2), visualized using the BioRad GelDoc™ and quantified by Azure™ software. h*TMX2*\_ex5–7 primers amplified the region from exon five through exon seven, h*TMX2*\_ex6–7 primers amplify the region between exon six and seven, and h*TMX2*\_ex6–8 primers amplify the region from exon six through exon eight.

## **RESULTS**

### **Identification of four consanguineous families segregating with microlissencephaly**

We studied eight affected individuals with neurological phenotypes consistent with microlissencephaly from four unrelated consanguineous families. Family 1673 presented with one affected child (1673-III-1) from a first-cousin marriage. The individual was born at full term with a significantly reduced head circumference (–2SD) and exhibited generalized tonic-clonic (GTC) seizures from birth (figure 1A, table 1). At her last evaluation, she exhibited severe intellectual disability, hypertonia, absence of motor skills, and increased deep tendon reflexes. Brain MRI revealed a thickened cerebral cortical mantle, with diminished gyral folds, with an appearance of pachygyria/lissencephaly, cortical atrophy, corpus callosum hypogenesis, and ventriculomegaly (figure 2A–B, supplementary figure S1A–C).

Family 2525 had two affected children (2525-III-2, and 2525-III-3) from a consanguineous marriage (figure 1B). Both children were born full term with significantly reduced head circumference (–3SD and –2SD, respectively). They also exhibited GTC seizures in the neonatal period with an onset of 2 weeks and 3 weeks, respectively. At their last evaluation, they were diagnosed with severe intellectual disability, increased deep tendon reflexes, delayed gross motor development, and absence of fine motor and language development (table 1). Brain MRI assessment of the older sibling revealed lissencephaly, reduced white matter volume, cortical atrophy, corpus callosum hypogenesis, and ventriculomegaly. (figure 2C–D, supplementary figure S1D–F).

Family 4984 had three affected children (4984-III-1, 4984-III-3, and 4984-III-4) and one healthy sibling from a consanguineous marriage (figure 1C). The oldest affected child was born at full term with a reduced head circumference (–1SD). He was also diagnosed with severe intellectual disability, delayed gross motor and language development, absent fine motor development, and epilepsy. He died at 5 years of age due to pneumonia. His younger two affected siblings (4984-III-3, and 4984-III-4) were both born at 36 weeks and showed reduced head circumference at last evaluation (–4SD and –3SD, respectively). They exhibited similar symptoms as their older sibling. Brain MRIs were obtained from one child (4984-III-3), and showed lissencephaly, corpus callosum hypoplasia, reduced white matter volume, ventriculomegaly, and cerebellar atrophy (figure 2E–F, supplementary figure S1G–I).

Family 3501 had two affected children (3501-III-6 and 3501-III-7) and five healthy siblings from a consanguineous marriage (figure 1D). Both affected individuals were born at full term with significantly reduced head circumferences ( $-2SD$ ). They also exhibited neonatal epilepsy, which predated their diagnoses of severe intellectual disability, delayed/absent psychomotor development, and increased tendon reflexes at last evaluation. Brain MRIs for both children showed lissencephaly, cerebral mantle thickening, ventriculomegaly, reduced white matter volume, cerebellar atrophy, and corpus callosum hypoplasia (figure 2G–H, supplementary figure S1J–O).

### Identification of a homozygous *TMX2* c.500G>A variant in families with microlissencephaly

Whole exome sequencing (WES) was performed on blood-derived DNA from the affected child in Family 1673. For variant identification Genome Analysis Toolkit (GATK) workflow identified variants that were intersected with identity-by-descent blocks from HomozygosityMapper.[18,19] Rare potentially deleterious variants were prioritized against an in-house exome database consisting of over 4,000 ethnically matched individuals, in addition to publicly available exome datasets, cumulatively numbering over 10,000 individuals. From this analysis, we identified three variants that passed these filter parameters in the genes *RAB3GAP2* (MIM:609275), *TMX2*, and *MOCOS* (MIM:613274) (see supplementary table S1). Patient phenotypes did not match the phenotypes reported for *RAB3GAP2* and *MOCOS*, leaving a single, homozygous hg38:Chr11:g.57739039G>A (GenBank: NM\_001347898.1) variant in *TMX2*, located at the last base of exon six of eight (c.500G>A), as the sole candidate. We then performed WES on one affected child each from Families 2525 and 4984, and both affected children from Family 3501, based on matching phenotypic features between the families. Interestingly, we identified the same *TMX2* variant recurring in all three families (supplementary table S1). Further, each of the four consanguineous families showed a run of homozygosity that contained *TMX2*, consistent with the parental consanguinity (figure 3), although the haplotype blocks showed no commonality of shared SNPs of any size (supplementary figure S2). This suggests that the variant arose independently in each family on separate haplotypes, or was so distantly derived that a common haplotype could not be identified. This variant was confirmed by direct Sanger sequencing analysis, and testing of all available family members demonstrated segregation with the phenotype according to a recessive mode of inheritance (supplementary figure S3). We found no additional families in our own cohort of over 5000 individuals, or in the GeneMatcher website, of patients displaying likely causative variants in this gene. The variant was also not identified in the Greater Middle Eastern (GME) Variome (consisting of 2,497 individuals) or any other public database.[20] These analyses made *TMX2* the top candidate for pathogenesis.

*TMX2* encodes for Thioredoxin-related transmembrane protein 2, and the variant introduced an amino acid substitution in the Trx-like domain of the protein (p.Arg205Gln, figure 4A–B). The p.Arg205Gln substitution was also predicted to be disease-causing by MutationTaster.[17] *TMX2* has two protein-coding isoforms, isoform 1 and 2 (NP\_001334827.1 and NP\_057043.1), which differ in the length of the Extracellular Topological Domain (TAD) and absence of the transmembrane domain in isoform 2 (figure 4B), but functional differences between these isoforms are not reported.

As this homozygous variant occurred in the last nucleotide of exon 6 (figure 4D), we considered a potential impact on *TMX2* splicing or mRNA stability. In addition to the two canonical protein-coding isoforms, *TMX2* is also predicted to undergo alternative splicing at the exon 6–7 junction, which is a particularly small intron. Approximately 95% of observed transcripts from NCBI conform to a 91 bp intron, with the amino acid sequence reading ... **DVSTRYKVS**.... One minor isoform, representing approximately 2% of transcripts, contains a 69 bp intron, with the sequence reading ...**DVSTRYELSGPCRYKVS**..., due to the use of an alternative 3' splice acceptor site. The other minor isoform, representing approximately 3% of transcripts, conforms to a 102 bp intron, with the sequence reading ... **DVQSE**... (figure 4E), yet contains a premature stop codon approximately 26 amino acids downstream, suggesting a non-functional isoform. Whether or not these isoforms are found in nature or encode for protein has yet to be elucidated.

### The *TMX2* c.500G>A mutation results in reduced mRNA levels in affected individuals

*TMX2* is ubiquitously expressed in adult human tissues (GTEx data, supplementary figure S4). Additionally, *TMX2* is expressed in human brain during development at all assessed stages (supplementary figure S5), consistent with a role in this phenotype. Because the variant alters the last base of an exon, we considered whether splicing or RNA stability could be impacted. Thus RNA was extracted from frozen whole blood obtained from the father and one affected individual from Family 2525 as well as both parents and one affected from Family 4984. mRNA transcript levels were assessed using RT-PCR across various regions flanking the variant (figure 5A) and compared to an unrelated control sample. Three primer pairs were designed: 1] the region between exons five and seven, 2] the region between exon six and seven, 3] the region between exons six and eight (figure 5B, supplementary table S2). We did not observe evidence of any novel splice isoforms, such as might result from exon skipping or intron inclusion; however, *TMX2* mRNA levels were reduced to 15–50% of control in both samples from affecteds compared with the healthy control, whereas unaffected obligate carriers showed levels between 50–90% of normal (figure 5C–D). The reduced mRNA levels in patients and carriers is consistent with an effect of *TMX2* c.500G>A on splicing or RNA stability, and the absence of novel bands in the affected and carrier individuals suggests nonsense mediated decay of aberrantly spliced mRNA.

### Lack of *C9ORF72* repeat expansion in *TMX2* mutated samples

*C9ORF72* gene mutations are the most common cause of Amyotrophic Lateral Sclerosis (ALS, MIM:105400) and Frontotemporal Dementia (FTD, MIM:600274).[20,21] The damaging mutation in *C9ORF72* associated with these diseases is an expanded noncoding hexanucleotide repeat (GGGGCC), leading to repeat-associated non-ATG (RAN) translation of a dipeptide repeat protein (DPR).[21,22] Previous transcriptomic analysis using *C9ORF72*-mutant ALS brain tissue revealed upregulation of genes involved in ER stress, [23] suggesting failed ER stress response in *C9ORF72* pathogenesis. Following a CRISPR-Cas9 KO screen for genetic modifiers of DPR toxicity, *TMX2* emerged as one of the two strongest protective modifier genes identified.[24] In these experiments, loss of *TMX2* suppressed the toxic effect of the *C9ORF72* DPR, suggesting that *TMX2* is an activator of

DPR toxicity. Therefore, we wanted to test the possibility that the *TMX2* mutation occurred in the genetic background of *C9ORF72* expansion.

To test this, we performed repeat-primed PCR using a previously validated detection method to screen all available DNA samples from three families for the presence of the GGGGCC hexanucleotide repeat expansion (Family 3501 failed analysis due to insufficient amounts of DNA available).[25] All remaining samples were absent for the expanded *C9ORF72* repeat, as compared to the negative control and an unrelated positive control sample (figure S6).

## DISCUSSION

Here we demonstrate a recurrent variant in *TMX2* associated with a severe, recessive neurological disease characterized by microcephaly with lissencephaly. All affected individuals in four families carried an identical homozygous c.500G>A variant in *TMX2* and displayed microlissencephaly, global developmental delay, intellectual disability, and epilepsy. The variant led to decreased mRNA steady-state levels, and was not associated with expansion in the *C9ORF72* hexanucleotide repeat. Our results implicate a relatively common single allele as a cause for microlissencephaly in humans.

*TMX2* is arguably the least studied member of the PDI family. *TMX2* was cloned in 2003, and encodes a multidomain transmembrane protein that is enriched on the mitochondria-associated membrane (MAM) of the ER via palmitoylation of two of its cystolically-exposed cysteines.[13,26] The MAM is a domain of the ER that mediates the exchange of ions, lipids and metabolites between the ER and mitochondria, suggesting a potential function in either mitochondria, ER, or both. *TMX2* shows ubiquitous expression, with highest levels detected in heart, brain, liver, kidney and pancreas.[12,13,27] Whether *TMX2* displays catalytic activity remains unclear, given that the canonical CXXC motif required for oxidoreductase activity is replaced by an SXXC motif.[28]

There was one prior mention of *TMX2* in human disease, where a cohort of patients with malformations of cortical development was sequenced to identify causes.[29] One family was identified with two children affected with lissencephaly where two candidate genes emerged, one being *TMX2*. [29] In this family, *TMX2* showed compound heterozygous mutations [(c.326A>G; p.Asp109Gly) and (c.691C>T; p.Arg231Trp)], but brain MRI was not available to allow comparisons with our cases. Our results, linking *TMX2* to lissencephaly, suggest that, in the previous family, *TMX2* was likely the relevant gene.

Mutations in genes that encode ER stress response proteins have been implicated in a range of neuroprogressive disorders among other human diseases, including Parkinson's disease, Huntington's disease, and ALS, the latter of which has been studied in connection with ER stress response pathways and apoptosis.[30–33] *TMX2* knockdown or CRISPR targeting was able to rescue the cell death and ER stress response toxicity induced by application of the DPR encoded by the *C9ORF72* expansion. CRISPR targeting of *TMX2* in DPR-expressing human cells showed upregulation of prosurvival unfolded-protein-response-pathway genes including *Atf3*, and downregulation of calcium-binding and apoptotic proteins.[24] We found no evidence of expansion of the *C9ORF72* repeat in patient cells,

suggesting that loss of *TMX2* was not secondary to effects of *C9ORF72*, but it is possible that the mutated *TMX2* allele is under positive selection, as it appears to have arisen independently on four separate haplotypes. It would be interesting as a next step to understand mechanism by generating an animal model of disease; however, initial attempts indicate that homozygous *Tmx2* null mutations in mouse are lethal prior to weaning, with complete penetrance.[34]

The presence of a Trx-like domain in *TMX2* suggests a role regulating redox pathways, specifically in relation to the ER stress response. Partial or complete loss of *TMX2* may thus predispose to cell death. While we have not linked the phenotypes from our cases to a molecular function in this study, increased ER stress during neurodevelopment has been linked to aberrant neuronal maturation and the subsequent development of neurodevelopmental disorders caused by abnormal neuronal differentiation and maturation. [35–36] We hypothesize that loss of *TMX2* in humans may lead to cell-death mediated depletion of neural progenitor cells in the developing cerebral cortex during embryogenesis, producing microlissencephaly. Whether correct, or whether there are secondary effects of *TMX2* in neurogenesis or neuronal migration, remain to be explored.

## Supplementary Material

Refer to Web version on PubMed Central for supplementary material.

## Acknowledgments

The authors thank the patients and their families for participation in this study. We would like to thank Grazia Mancini for communicating unpublished results. The Genotype-Tissue Expression (GTEx) Project was supported by the Common Fund of the Office of the Director of the National Institutes of Health, and by NCI, NHGRI, NHLBI, NIDA, NIMH, and NINDS. The data used for the analyses described in this manuscript were obtained from: the GTEx Portal on 03/03/2018.

**Funding:** S.G. was sponsored by the Ruth L. Kirschstein Institutional National Research Service Award (T32 GM008666) from the National Institute on Deafness and Other Communication Disorders and by award F31HD095602 from the NIH Eunice Kennedy Shriver National Institute of Child Health and Human Development. We thank the Broad Institute (U54HG003067 to E. Lander and UM1HG008900 to D. MacArthur) and the Yale Center for Mendelian Disorders (U54HG006504 to M. Gunel). This work was supported by NIH grants R01NS048453, R01NS052455, the Simons Foundation Autism Research Initiative and Howard Hughes Medical Institute (to J.G.G.). This work was supported in part by the Intramural Research Programs of the NIH, National Institute on Aging (Z01-AG000949-02 to B.J. Traynor).

## REFERENCES

1. Fry AE, Cushion TD, Pilz DT. The genetics of lissencephaly. *Am J Med Genet C Semin Med Genet* 2014;166C:198–210. [PubMed: 24862549]
2. Zaki M, Shehab M, El-Aleem AA, Abdel-Salam G, Koeller HB, Ilkin Y, Ross ME, Dobyns WB, Gleeson JG. Identification of a novel recessive *RELN* mutation using a homozygous balanced reciprocal translocation. *Am J Med Genet* 2007;143A:939–944. [PubMed: 17431900]
3. Alkuraya FS, Cai X, Emery C, Mochida GH, Al-Dosari MS, Felie JM, Hill RS, Barry BJ, Partlow JN, Gascon GG, Kentab A, Jan M, Shaheen R, Feng Y, Walsh CA. Human mutations in *NDE1* cause extreme microcephaly with lissencephaly. *Am J Hum Genet* 2011;88:536–547. [PubMed: 21529751]
4. Radmanesh F, Caglayan AO, Silhavy JL, Yilmaz C, Cantagrel V, Omar T, Rosti B, Kaymakcalan H, Gabriel S, Li M, Sestan N, Bilguvar K, Dobyns WB, Zaki MS, Gunel M, Gleeson JG. Mutations in

LAMB 1 cause cobblestone brain malformation without muscular or ocular abnormalities. *Am J Hum Genet* 2013;92:468–474. [PubMed: 23472759]

5. Mishra-Gorur K, Ça layan AO, Schaffer AE, Chabu C, Henegariu O, Vonhoff F, Akgümü GT, Nishimura S, Han W, Tu S, Baran B, Gümü H, Dilber C, Zaki MS, Hossni HA, Rivière JB, Kayserili H, Spencer EG, Rosti RÖ, Schroth J, Per H, Ça lar C, Ça lar Ç, Dölen D, Baranoski JF, Kumanda S, Minja FJ, Erson-Omay EZ, Mane SM, Lifton RP, Xu T, Keshishian H, Dobyns WB, Chi NC, Šestan N, Louvi A, Bilgüvar K, Yasuno K, Gleeson JG, Günel M. Mutations in *KATNB1* cause complex cerebral malformations by disrupting asymmetrically dividing neural progenitors. *Neuron* 2014;84:1226–39. [PubMed: 25521378]
6. Magen D, Ofir A, Berger L, Goldsher D, Eran A, Katib N, Nijem Y, Vlodavsky E, Tzur S, Behar DM, Fellig Y, Mandel H. Autosomal recessive lissencephaly with cerebellar hypoplasia is associated with a loss-of-function mutation in *CDK5*. *Hum Genet* 2015;134: 305–314. [PubMed: 25560765]
7. Jerber J, Zaki MS, Al-Aama JY, Rosti RO, Ben-Omran T, Dikoglu E, Silhavy JL, Caglar C, Musaev D, Albrecht B, Campbell KP, Willer T, Almurieki M, Caglayan AO, Vajsar J, Bilguvar K, Ogur G, Abou Jamra R, Gunel M, Gleeson JG. Biallelic mutations in *TMTTC3*, encoding a transmembrane and TPR-containing protein, lead to cobblestone lissencephaly. *Am J Hum Genet* 2016;99:1181–1189. [PubMed: 27773428]
8. Faheem M, Naseer MI, Rasool M, Chaudhary AG, Kumosani TA, Ilyas AM, Pushparaj P, Ahmed F, Algahtani HA, Al-Qahtani MH, Saleh Jamal H. Molecular genetics of human primary microcephaly: an overview. *BMC Med Genomics* 2015;8:S4.
9. Barkovich AJ, Ferriero DM, Barr RM, Gressens P, Dobyns WB, Truwit CL, Evrard P. Microlissencephaly: a heterogeneous malformation of cortical development. *Neuropediatrics* 1998;29:113–9. [PubMed: 9706619]
10. Parrini E, Conti V, Dobyns WB, Guerrini R. Genetic Basis of Brain Malformations. *Mol Syndromol* 2016;7:220–233. [PubMed: 27781032]
11. Racape M, Van Huyen JPD, Danger R, Giral M, Bleicher F, Foucher Y, Pallier A, Pilet P, Tafelmeyer P, Ashton-Chess J, Dugast E, Pettre S, Charreau B, Soullillou JP, Brouard S. The involvement of *SMILE/TMTTC3* in endoplasmic reticulum stress response. *PLoS One* 2011;6:e19321. [PubMed: 21603654]
12. Nakagawa T, Zhu H, Morishima N, Li E, Xu J, Yankner BA, Yuan J. Caspase-12 mediates endoplasmic-reticulum-specific apoptosis and cytotoxicity by amyloid-beta. *Nature* 2000;403:98–103. [PubMed: 10638761]
13. Meng X, Zhang C, Chen J, Peng S, Cao Y, Ying K, Xie Y, Mao Y. Cloning and identification of a novel cDNA coding thioredoxin-related transmembrane protein 2. *Biochem Genet* 2003;41:99–106. [PubMed: 12670024]
14. Matsusaki M, Kanemura S, Kinoshita M, Lee YH, Inaba K, Okumura M. The Protein Disulfide Isomerase Family: from proteostasis to pathogenesis. *Biochim Biophys Acta Gen Subj* 2019;19:30080–7.
15. Dixon-Salazar TJ, Silhavy JL, Udpa N, Schroth J, Bielas S, Schaeffer AE, Olvera J, Bafna V, Zaki MS, Abdel-Salam GH, Mansour LA, Selim L, Abdel-Hadi S, Marzouki N, Ben-Omran T, Al-Saana NA, Sonmez FM, Celep F, Azam M, Hill KJ, Collazo A, Fenstermaker AG, Novarino G, Akizu N, Garimella KV, Sougnez C, Russ C, Gabriel SB, Gleeson JG. Exome sequencing can improve diagnosis and alter patient management. *Sci Transl Med* 2012;4:138ra78.
16. Seelow D, Schuelke M. HomozygosityMapper 2012--bridging the gap between homozygosity mapping and deep sequencing. *Nucleic Acids Res* 2012;40:W516–520. [PubMed: 22669902]
17. Schwarz JM, Rodelsperger C, Schuelke M, Seelow D. MutationTaster evaluates disease-causing potential of sequence alterations. *Nat Methods* 2010;7:575–576. [PubMed: 20676075]
18. Seelow D, Schuelke M, Hildebrandt F, Nurnberg P. HomozygosityMapper--an interactive approach to homozygosity mapping. *Nucleic Acids Res* 2009;37:W593–599. [PubMed: 19465395]
19. Scott EM, Hales A, Itan Y, Spencer EG, He Y, Azab MA, Gabriel SB, Belkadi A, Boisson B, Abel L, Clark AG, Greater Middle East Variome Consortium, Alkuraya FS, Casanova JL, Gleeson JG. Characterization of Greater Middle Eastern genetic variation for enhanced disease gene discovery. *Nat Genet* 2016;48:1071–1076. [PubMed: 27428751]

20. DePristo MA, Banks E, Poplin RE, Garimella KV, Maguire JR, Hartl C, Philippakis AA, del Angel G, Rivas MA, Hanna M, McKenna A, Fennell TJ, Kernysky AM, Sivachenko AY, Cibulskis K, Gabriel SB, Altshuler D, Daly MJ. A framework for variation discovery and genotyping using next-generation DNA sequencing data. *Nat Genet* 2011;43:491–498. [PubMed: 21478889]
21. DeJesus-Hernandez M, Mackenzie IR, Boeve BF, Boxer AL, Baker M, Rutherford NJ, Nicholson AM, Finch NA, Flynn H, Adamson J, Kouri N, Wojtas A, Sengdy P, Hsiung GY, Karydas A, Seeley WW, Josephs KA, Coppola G, Geschwind DH, Wszolek ZK, Feldman H, Knopman DS, Petersen RC, Miller BL, Dickson DW, Boylan KB, Graff-Radford NR, Radsemakers R. Expanded GGGGCC hexanucleotide repeat in noncoding region of C9ORF72 causes chromosome 9p-linked FTD and ALS. *Neuron* 2011;72:245–256. [PubMed: 21944778]
22. Renton AE, Majounie E, Waite A, Simón-Sánchez J, Rollinson S, Gibbs JR, Schymick JC, Laaksovirta H, van Swieten JC, Myllykangas L, Kalimo H, Paetau A, Abramzon Y, Remes AM, Kaganovich A, Scholz SW, Duckworth J, Ding J, Harmer DW, Hernandez DG, Johnson JO, Mok K, Ryten M, Trabzuni D, Guerreiro RJ, Orrell RW, Neal J, Murray A, Pearson J, Jansen IE, Sondervan D, Seelaar H, Blake D, Young K, Halliwell N, Callister JB, Toulson G, Richardson A, Gerhard A, Snowden J, Mann D, Neary D, Nalls MA, Peuralinna T, Jansson L, Isoviita VM, Kaivorinne AL, Hölttä-Vuori M, Ikonen E, Sulkava R, Benatar M, Wu J, Chiò A, Restagno G, Borghero G, Sabatelli M; ITALSGEN Consortium, Heckerman D, Rogaeva E, Zinman L, Rothstein JD, Sendtner M, Drepper C, Eichler EE, Alkan C, Abdullaev Z, Pack SD, Dutra A, Pak E, Hardy J, Singleton A, Williams NM, Heutink P, Pickering-Brown S, Morris HR, Tienari PJ, Traynor BJ. A hexanucleotide repeat expansion in C9ORF72 is the cause of chromosome 9p21-linked ALS-FTD. *Neuron* 2011;72:257–268. [PubMed: 21944779]
23. Prudencio M, Belzil VV, Batra R, Ross CA, Gendron TF, Pregent LJ, Murray ME, Overstreet KK, Piazza-Johnston AE, Desaro P, Bieniek KF, DeTure M, Lee WC, Biendarra SM, Davis MD, Baker MC, Perkerson RB, van Blitterswijk M, Stetler CT, Rademakers R, Link CD, Dickson DW, Boylan KB, Li H, Petrucelli L. Distinct brain transcriptome profiles in C9orf72-associated and sporadic ALS. *Nat. Neurosci* 2015;18:1175–1182. [PubMed: 26192745]
24. Kramer NJ, Haney MS, Morgens DW, Jovi A, Couthouis J, Li A, Ousey J, Ma R, Bieri G, Tsui CK1, Shi Y, Hertz NT, Tessier-Lavigne M, Ichida JK, Bassik MC, Gitler AD. CRISPR-Cas9 screens in human cells and primary neurons identify modifiers of C9ORF72 dipeptide-repeat-protein toxicity. *Nat Genet* 2018;60:603–612.
25. Renton AE, Majounie E, Waite A, Simón-Sánchez J, Rollinson S, Gibbs JR, Schymick JC, Laaksovirta H, van Swieten JC, Myllykangas L, Kalimo H, Paetau A, Abramzon Y, Remes AM, Kaganovich A, Scholz SW, Duckworth J, Ding J, Harmer DW, Hernandez DG, Johnson JO, Mok K, Ryten M, Trabzuni D, Guerreiro RJ, Orrell RW, Neal J, Murray A, Pearson J, Jansen IE, Sondervan D, Seelaar H, Blake D, Young K, Halliwell N, Callister JB, Toulson G, Richardson A, Gerhard A, Snowden J, Mann D, Neary D, Nalls MA, Peuralinna T, Jansson L, Isoviita VM, Kaivorinne AL, Hölttä-Vuori M, Ikonen E, Sulkava R, Benatar M, Wu J, Chiò A, Restagno G, Borghero G, Sabatelli M; ITALSGEN Consortium, Heckerman D, Rogaeva E, Zinman L, Rothstein JD, Sendtner M, Drepper C, Eichler EE, Alkan C, Abdullaev Z, Pack SD, Dutra A, Pak E, Hardy J, Singleton A, Williams NM, Heutink P, Pickering-Brown S, Morris HR, Tienari PJ, Traynor BJ. A hexanucleotide repeat expansion in C9ORF72 is the cause of chromosome 9p21-linked ALS-FTD. *Neuron* 2011;72:257–268. [PubMed: 21944779]
26. Lynes EM, Bui M, Yap MC, Benson MD, Schneider B, Ellgaard L, Berthiaume LG, Simmen T. Palmitoylated TMX and calnexin target to the mitochondria-associated membrane. *EMBO J* 2012;31:451–70.
27. Galligan JJ, Petersen DR. The human protein disulfide isomerase gene family. *Hum Genomics* 2012;6:6. [PubMed: 23245351]
28. Ellgaard L, Ruddock LW. The human protein disulphide isomerase family: substrate interactions and functional properties. *EMBO Rep* 2005;6:28–32. [PubMed: 15643448]
29. Zillhaardt JL, Poirier K, Broix L, Lebrun N, Elmorjani A, Martinovic J, Saillour Y, Muraca G, Nectoux J, Bessieres B, Fallet-Biano C, Lyonnet S, Dulac O, Odent S, Rejeb I, Ben Jemaa L, Rivier F, Pinson L, Genevieve D, Musizzano Y, Bigi N, Leboucq N, Giuliano F, Philip N, Vilain C, Van Bogaert P, Maurey H, Beldjord C, Artiguenave F, Boland A, Olasso R, Masson C, Nitschke P, Deleuze JF, Bahi-Buisson N, Chelly J. Mosaic parental germline mutations causing recurrent forms of malformations of cortical development. *Eur J Hum Genet* 2016;4:611–4.

30. Kaiser BK, Yim D, Chow IT, Gonzalez S, Dai Z, Mann HH, Strong RK, Groh V, Spies TD. Disulphide-isomerase-enabled shedding of tumour-associated NKG2D ligands. *Nature* 2007;447:482–486. [PubMed: 17495932]
31. Hoffstrom BG, Kaplan A, Letso R, Schmid RS, Turmel GJ, Lo DC, Stockwell BR. Inhibitors of protein disulfide isomerase suppress apoptosis induced by misfolded proteins. *Nat Chem Biol* 2010;6:900–906. [PubMed: 21079601]
32. Atkin JD, Farg MA, Turner BJ, Tomas D, Lysaght JA, Nunan J, Rembach A, Nagley P, Beart PM, Cheema SS, Horne MK. Induction of the unfolded protein response in familial amyotrophic lateral sclerosis and association of protein-disulfide isomerase with superoxide dismutase 1. *J Biol Chem* 2006;281:30152–30165. [PubMed: 16847061]
33. Benham AM. The Protein Disulfide Isomerase Family: Key Players in Health and Disease. *Antioxid Redox Signal* 2012;16:781–89. [PubMed: 22142258]
34. <https://www.mousephenotype.org/data/genes/MGI:1914208>, month accessed: June 2019.
35. Kawada K, Lekumo T, Kaneko M, Nomura Y, Okuma Y. ER stress-induced aberrant neuronal maturation and neurodevelopmental disorders. *Yakugaku Zasshi* 2016;136:811–5. [PubMed: 27252060]
36. Breuss MW, Nguyen A, Song Q, Nguyen T, Stanley V, James KN, Musaev D, Chai G, Wirth SA, Anzenberg P, George RD, Johansen A, Ali S, Zia-Ur-Rehman M, Sultan T, Zaki MS, Gleeson JG. Mutations in LNPK, Encoding the Endoplasmic Reticulum Junction Stabilizer Lunapark, Cause a Recessive Neurodevelopmental Syndrome. *Am J Hum Genet* 2018;103:296–304. [PubMed: 30032983]

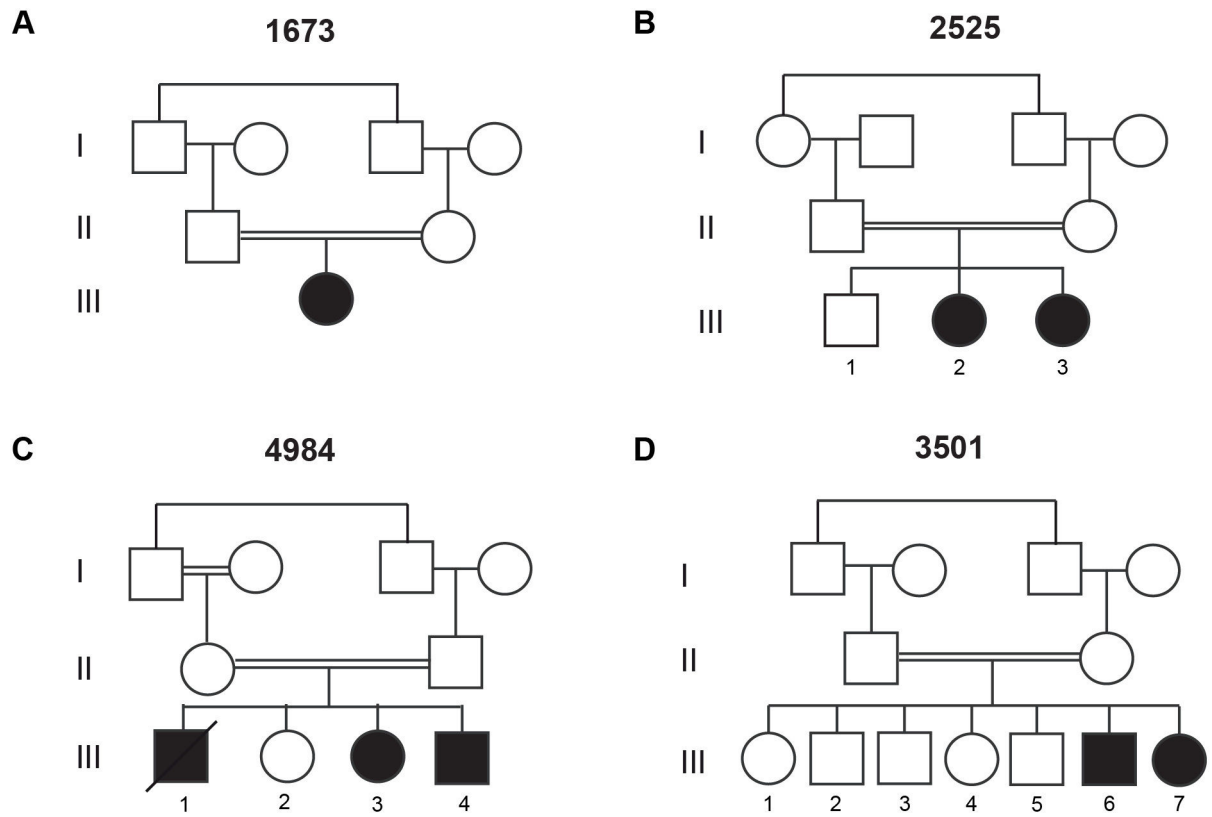


**Figure 1. Consanguineous families with a homozygous recessive mutation in *TMX2*.**  
 (A-D) Pedigrees of all four families showing first-cousin consanguineous marriages (double bar) with a total of eight affected children. All unfilled members are without neurological disease.

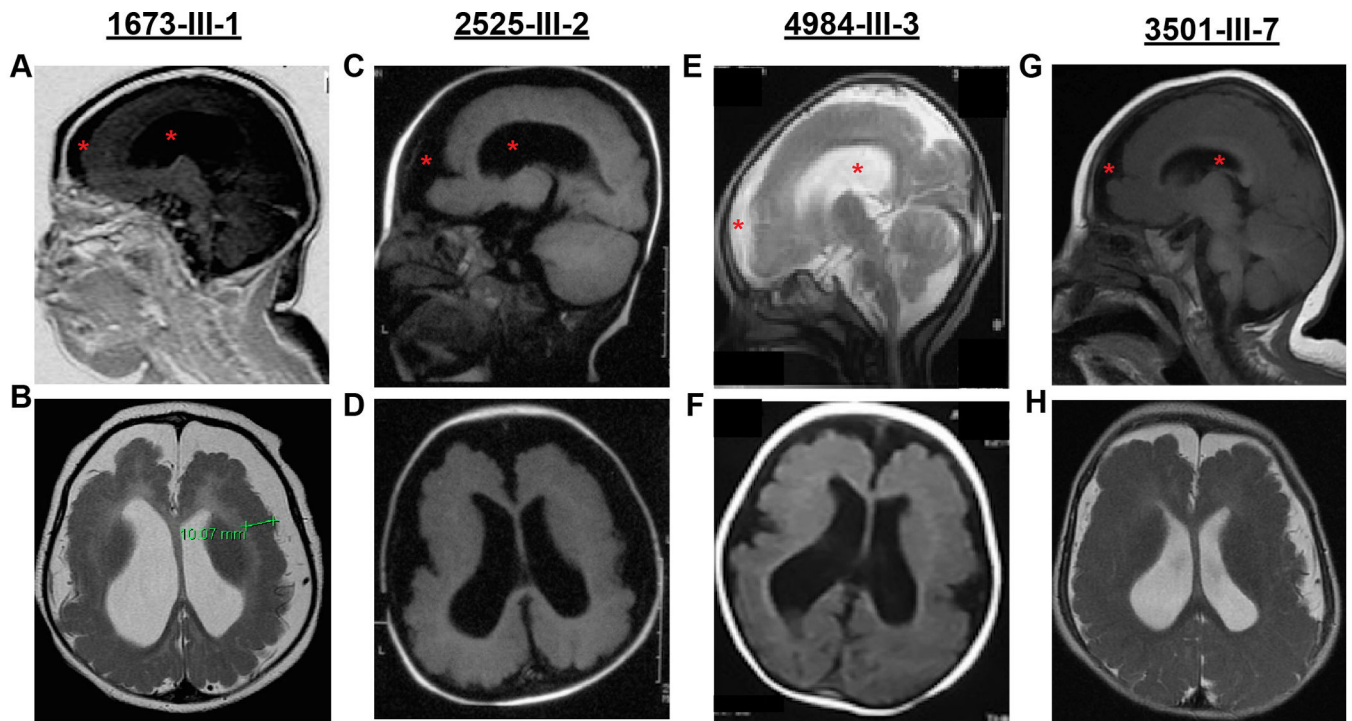


**Figure 2. MRIs from affected children display lissencephaly, microcephaly, and brain atrophy.** Top row: Midline sagittal MRI. Bottom row: Axial MRI. Subject ID provided at top. All images are T1-weighted except (B, E, H) which are T2 weighted, selected to best demonstrate the main imaging defects. The lack of cortical folding is apparent in both frontal and occipital regions, consistent with lissencephaly. Red asterisk in top row highlights ventriculomegaly and increased extra-axial fluid accumulation, consistent with brain atrophy and microcephaly. Bottom row shows paucity of cortical gyri and thickened gray matter, which was measured at 10.07 mm (green bracket) in (B), which is roughly twice the width of normal.

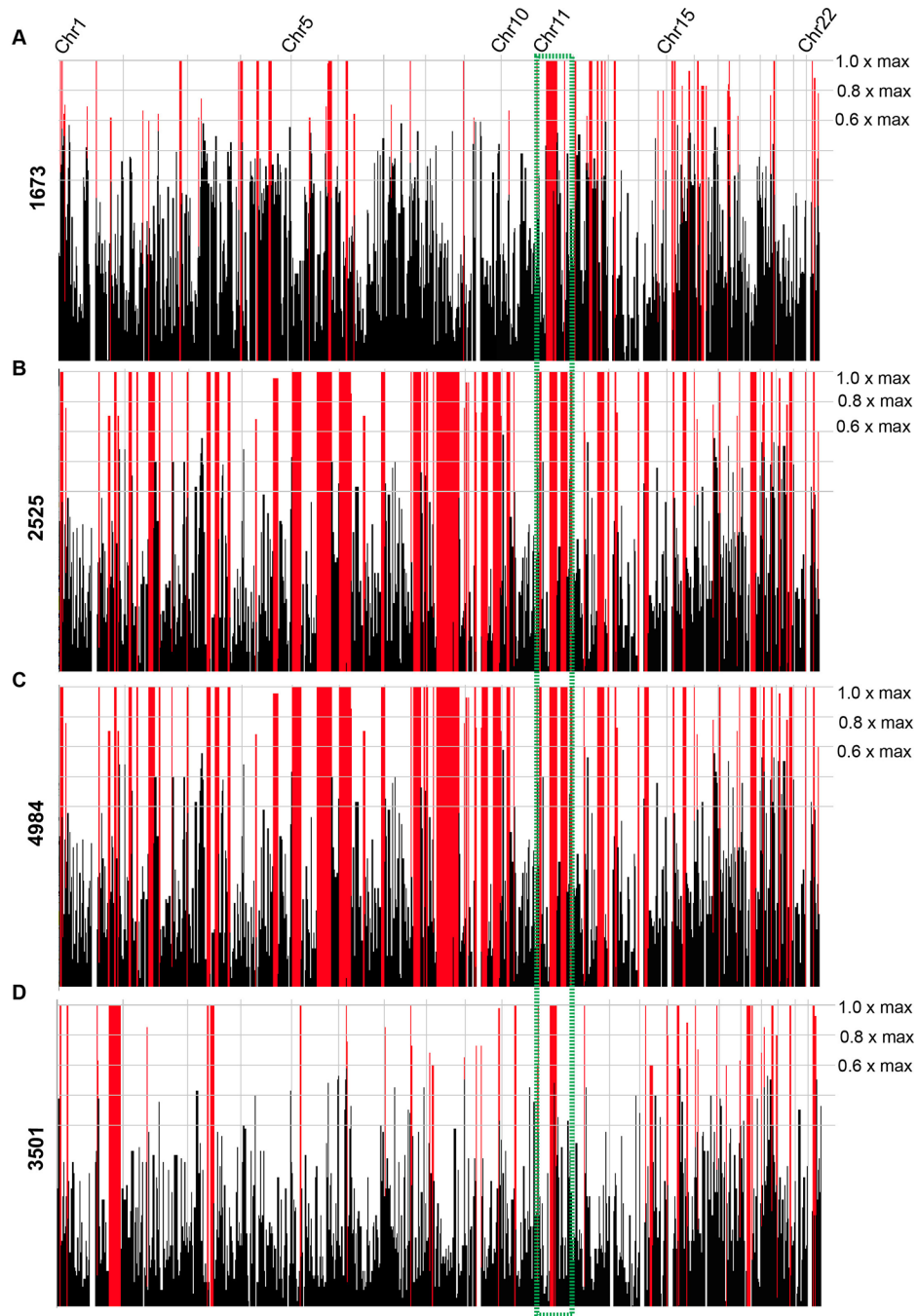


**Figure 3. Homozygosity plots for all four families display homozygosity surrounding the *TMX2* gene.**

(A-D) Graphical representation of regions of homozygosity, generated by HomozygosityMapper for all 22 autosomes for the affected individual in Family 1673 (III-1, A), one affected individual from Family 2525 (III-2, B), one affected individual from Family 4984 (III-3, C), and both affected individuals from Family 3501 (III-6 and III-7, D). Red peaks indicate homozygosity scores above the given cutoff at 0.8x of the maximum. All plots show a region of homozygosity containing the *TMX2* gene (green box).

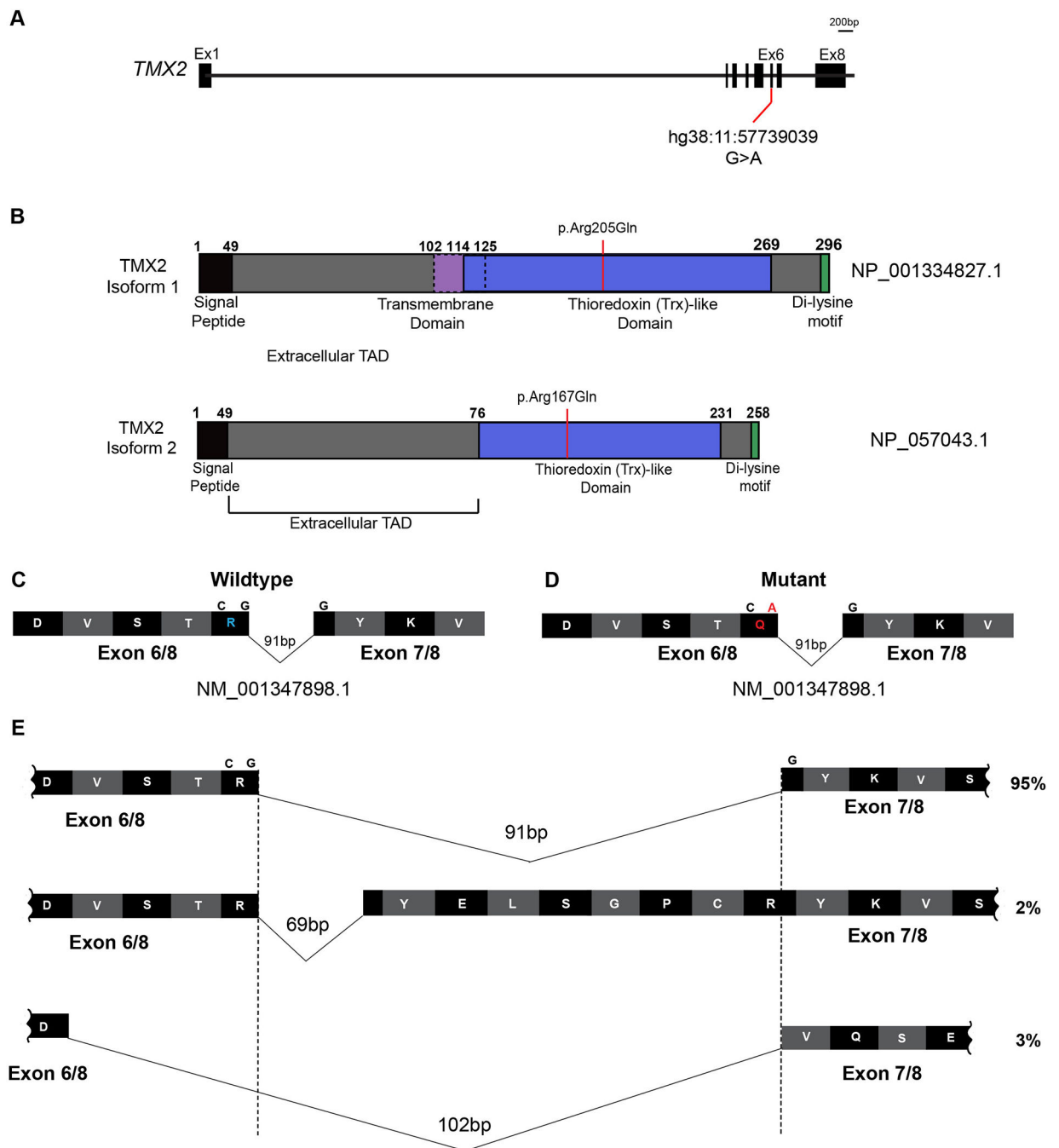


**Figure 4. *TMX2* gene and predicted protein isoforms.**

(A) Schematic of *TMX2* depicting the genomic map spanning eight exons. Red line indicates the position of the identified variant in exon six in all four families and coordinates within the cDNA map (RefSeq NM\_001347898.1). (B) Schematic of the two protein-coding isoforms of Thioredoxin-related transmembrane protein 2 (*TMX2*) depicting the location of the ‘signal peptide’ (black), extracellular topological associated domain (TAD), transmembrane domain (purple), Thioredoxin (Trx)-like domain (blue), and Di-lysine motif (green). Isoform 2 is 38 amino acids shorter than isoform 1 due to absence of the

transmembrane domain and part of the extracellular TAD. Red line indicates the position and coordinates of the amino acid change in affected individuals from all four families within the Trx-like domain. (C-D) Illustration of partial wildtype (C) and mutant (D) residues from exons six and seven surrounding the variant shown in blue and red in wildtype and mutant, respectively. (E) Schematic of the additional splice isoforms of the exon6–7 junction of *TMX2*, based on the UCSC Genome Browser with predicted percent existence of each isoform in human tissues from GenBank. The percentage of each isoform was calculated based on the average number of Expressed Sequence Tags (ESTs) available, displaying that particular isoform (e.g. BI764082, BG170274, and BI561678, respectively).

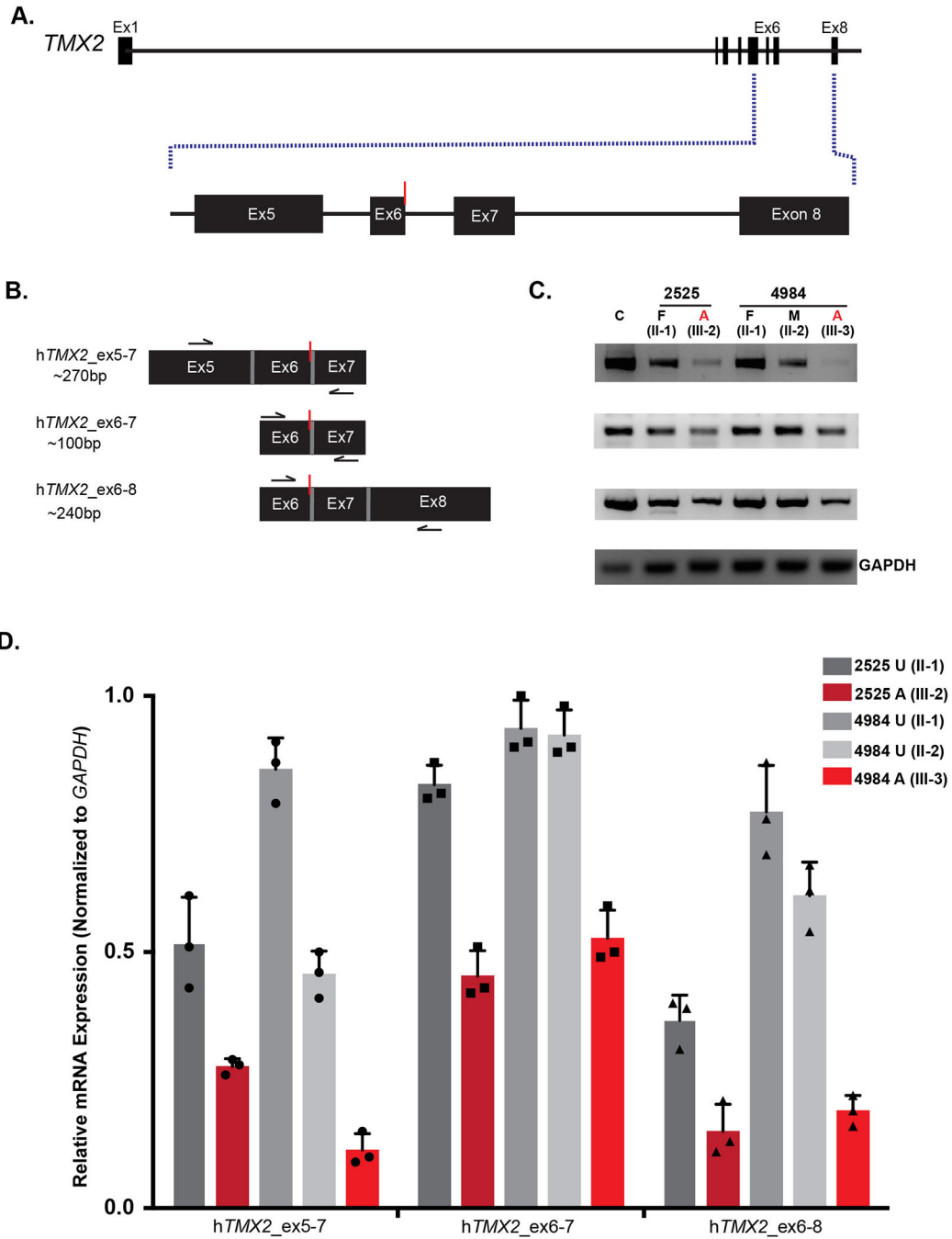


**Figure 5. *TMX2* c.500G>A allele associates with reduced mRNA levels in carriers and affected individuals.**

(A) Illustration of *TMX2* with an expanded view of exons five through eight. Red line indicates the location of the variant. (B) Schematic of primer pairs designed for RT-PCR analysis and expected base pair sizes for the corresponding products. Black arrows indicate the approximate location of the primers. Red line indicates the location of the variant. (C) RT-PCR analysis of RNA extracted from whole blood derived from an unrelated control (C), the unaffected father (II-1) and one affected individual (III-2) from Family 2525, and both parents (II-1 and II-2) and one affected individual (III-3) from Family 4984. There was

reduction of *TMX2* mRNA levels in affected individuals (red) compared to the normalized expression of 1.0 in the unrelated control (n=3). *TMX2* levels of parent carriers (grey) that were intermediate compared with unrelated control. *GAPDH* was used as a loading control. (D) Quantification of RT-PCR results displaying relative mRNA expression normalized to *GAPDH*. n=3 independent experiments. Bars show mean  $\pm$  standard deviation (SD) and individual data points.

**Table 1.****Clinical Table**

Clinical representation for affected subjects from all four families. Y:Yes. N:No. N/A: no data available. SD: standard deviations (calculated using SimulConsult's measurement resources). HC: head circumference. EEG: Electroencephalogram. EMG: electromyography

	Family 1673	Family 2525		Family 4984			Family 3501	
Individual	III-1	III-2	III-3	III-1	III-3	III-4	III-6	III-7
Gender	F	F	F	M	F	M	M	M
Country of Origin	Saudi Arabia	Pakistan		Egypt			Kuwait	
Parental Consanguinity	Y	Y		Y			Y	
Current age (if alive)	11y	N/A	6y	N/A	3y	2y	8y	6y
Age of death	N/A	4y	N/A	5y	N/A	N/A	N/A	N/A
Circumstances of death	N/A	Seizures	N/A	Pneumonia	N/A	N/A	N/A	N/A
<b>Mutation</b>								
Genomic (hg38)	Chr11:g.57739039G>A	Chr11:g.57739039G>A		Chr11:g.57739039G>A			Chr11:g.57739039G>A	
cDNA	c.500G>A	c.500G>A		c.500G>A			c.500G>A	
Protein	p.Arg205Gln	p.Arg205Gln		p.Arg205Gln			p.Arg205Gln	
Zygosity	homozygous	homozygous		homozygous			homozygous	
<b>Perinatal History</b>								
Pregnancy duration (weeks)	full term	full term	full term	full term	36w	36w	full term	full term
Weight at birth (g)	2990g	3300g	3200g	3100g	2800g	2900g	3100g	3100g
HC at birth (SD)	-2SD	-3SD	-2SD	-1SD	NA	-2SD	-2SD	-2SD
Age at last examination	11y	7y	5y	4y	2y	1y	8y	6y
Weight at last examination (kg)	20kg	17kg	10kg	11kg	8kg	7kg	22kg	12kg
Height at last examination (cm)	125cm	112cm	90 cm	92cm	75cm	65cm	110cm	85cm
HC at last examination (SD)	-3SD	-3SD	-4SD	-4SD	-3SD	-4SD	-4SD	-3SD
<b>Psychomotor development</b>								
Gross motor (normal/delayed/absent)	Absent	Delayed	Delayed	Delayed	Delayed	Absent	Delayed	Absent
Fine motor (normal/delayed/absent)	Absent	Absent	Absent	Absent	Absent	Absent	Absent	Absent
Language (normal/delayed/absent)	Absent	Absent	Absent	Delayed (babbling)	Absent	Delayed (babbling)	Absent	Delayed

	Family 1673	Family 2525			Family 4984			Family 3501	
Individual	III-1	III-2	III-3	III-1	III-3	III-4	III-6	III-7	
Social (normal/delayed/absent)	Absent	Delayed	Absent	Absent	Absent	Absent	Absent	Delayed	
<b>Seizures</b>									
Age of Onset	Neonatal	2w	3w	1m	1m	6w	2m	2m	
Type	GTC								
Frequency	2/w	2/w	1/w	1/m	1/m	2/m	4/m	2/m	
Controlled/Refractory	Refractory								
EEG	Multifocal spike/wave								
<b>Neuroimaging</b>									
Lissencephaly spectrum	Y	Y	Y	N/A	Y	N/A	Y	Y	
Cerebral mantle thickening	Y	N	N	N/A	N	N/A	Y	Y	
Subcortical band heterotopia	N	N	N	N/A	N	N/A	N	N	
Corpus callosum hypogenesis	Y	Y	Y	N/A	Y	N/A	Y	Y	
Cerebellar atrophy	N	N	N	N/A	Y	N/A	Y	Y	
Brainstem hypoplasia	N	N	N	N/A	Y	N/A	Y	Y	
Ventriculomegaly	Y	Y	Y	N/A	Y	N/A	Y	Y	
Reduced white matter	Y	Y	Y	N/A	Y	N/A	Y	Y	
<b>Neurological Examination</b>									
Intellectual disability (mild/moderate/severe)	Severe								
Hypertonia	Y	Y	Y	Y	Y	Y	Y	Y	
Hypotonia	N	N	N	N	N	N	N	N	
Deep tendon reflexes	Increased								
Spastic tetraplegia	Y	Y	Y	Y	Y	Y	Y	Y	
Ataxia	N	N	N	N	N	N	N	N	
EMG/Biopsy	N/A	N/A	N/A	N/A	EMG normal	EMG normal	N/A	N/A	
<b>Sensory</b>									
Vision	Fixes/Follows								
Hearing	Responds to noise								
<b>Other Clinical Features</b>									

	Family 1673	Family 2525		Family 4984			Family 3501	
Individual	III-1	III-2	III-3	III-1	III-3	III-4	III-6	III-7
Dysmorphism	N	N	N	N	N	N	N	N

Author Manuscript

Author Manuscript

Author Manuscript

Author Manuscript